2015 ASIA-PACIFIC
SOLAR RESEARCH CONFERENCE

Ingrid Haedrich

Cell to module (CTM) ratios for varying industrial cell types

Ingrid Haedrich[1], Sachin Surve[1] and Andrew Thomson[1]

[1]*Centre for Sustainable Energy Systems, ANU, Canberra, Australia*

E-mail: ingrid.haedrich@anu.edu.au

Abstract

Embedding solar cells into a solar module has an impact on the amount of light which can be absorbed by the solar cell. In a first matter it generates optical losses by absorbing and reflecting the irradiated sun light in or at the covering layer (e.g. glass and EVA). But there are also optical gains, which arise by embedding the cell in a material with an intermediate refractive index, which lies between the one of air and the cell surface. In this research we show that this coupling gain is strongly influenced by the reflectance of the cell measured against air. We investigate several industrial available solar cells types, which vary strongly in their surface structure (iso textures, inverted and random pyramids) and in their efficiency. We find that the change in short circuit current (ΔIsc), generated by embedding the solar cells in the same standard encapsulant (EVA) varies between -1.36% for multi crystalline to -6.5 % for high efficient IBC solar cells. Further we demonstrate how this impacts the cell to module ratio (CTM) by calculating the resulting module power for an industrial sized module configuration. Based on this we discuss the CTM ratios which can be achieved for a certain cell technology.

1. Introduction

On the way from a single solar cell to a complete module, efficiency losses in the range of 10-15 percent relative are observed. This high total loss results from a combination of various loss and gain mechanisms.

Between the module layers there are several optical effects interacting with each other. Starting with the glass, optical losses result from the effective reflectivity of the air-glass interface. It depends on the material refractive index, the surface structures and possibly the antireflective coating. The bulk absorptions of the glass and EVA material generate further optical losses.

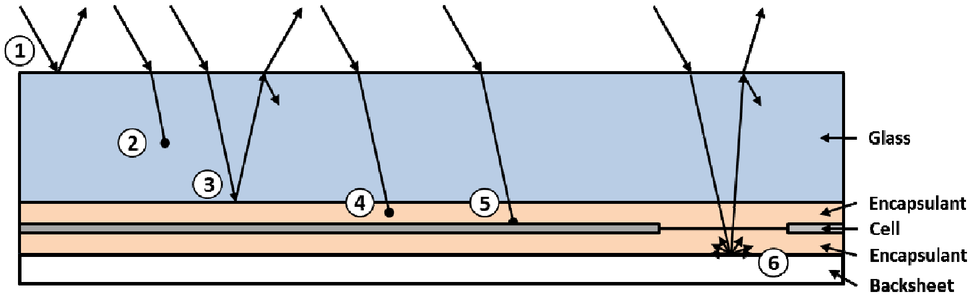

Figure 1 Illustration of optical effects in module. The sketch is modified from [1]

The optical coupling gains can be separated in direct in indirect gain mechanisms. A direct coupling gain may arise due to the fact that the cell was formerly characterized in an air environment with a refractive index of 1, whereas in a common module built-up it is optically coupled to an encapsulant with an index in the range of 1.5. This coupling reduces the index gap at the top interface of a simple AR-coating with a refractive index in the range of 2.1, thus reducing the reflectance of this interface. The coupling also reduces the reflectance of the entire stack (encapsulant/AR-coating/wafer), which can be confirmed by coherent reflectance calculations. The direct coupling gain depends strongly on the AR coating design.

The indirect coupling describes the effect that light which is reflected at the active cell surface, finger, ribbons and on the backsheet between the cells may be redirected at the glass/air interface back to the active cell area, especially by total internal reflection. In case of a non-embedded solar cell the reflected light at the cell front cannot be recoupled and is therefore lost.

In this work we will focus on the determination of direct and indirect coupling effects for three varying cell types in a first step. Further we use these measurement results as input for a calculation model [2] to predict the module power and efficiency. This enables an detailed comparison of cell to module ratios for the three cell concepts.

2. Determination of coupling gains

Cell efficiency is measured typically against air. By encapsulating the cell with a material of intermediate refraction index, a current gain due to coupling effects has to be considered. Coupling effects include reduced reflectivity of the active area and additional total reflection gains affecting reflections from the active cell area, the fingers and partially the busbar ribbon.

The determination of the optical coupling gains at the front surface of a cell starts by measuring the initial short circuit current $I_{sc,air}$ of single solar cells, contacted with cell connector ribbons, against air under STC conditions. Afterwards the same cells are encapsulated with one layer of the embedding material and a high absorptive black back sheet material. Then the short circuit current $I_{sc,encap}$ of the encapsulated sample is measured again.

The following cell types are investigated:

Table 1: Investigated solar cell types

cell type	*description*	*cell efficiency/ power*
multi crystalline	Isotextured, coated, 3 busbars, 6 inch, full square	17.7%, 4.31Wp
mono crystalline, PERC	Random pyramids, coated, 3 busbars, 6 inch, pseudo square	20.2%, 4.83Wp
IBC, mono crystalline	Radom pyramids, coated, no BB, no front metallization 5 inch, pseudo square	22.14%, 3.29Wp

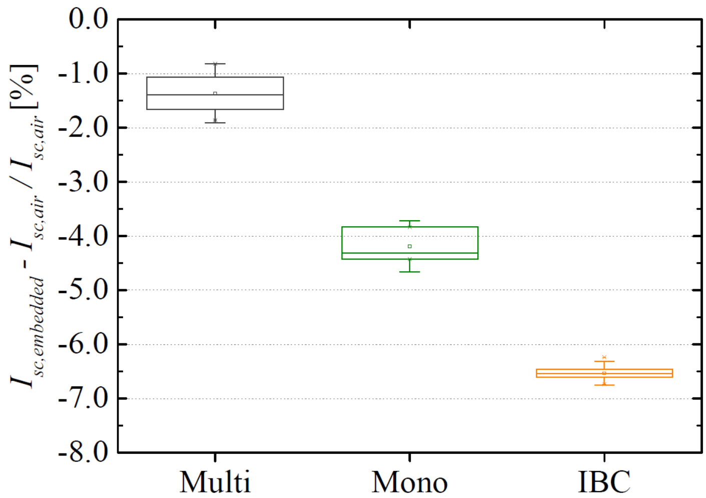

Figure 2 Percentage change of short circuit current for different types of solar cells, which are encapsulated using a standard EVA and a black backsheet. The solar cells are sorted from left to right according to their decreasing reflectance of front texture and coating.

With a decreasing reflectance of the cell surface (left to right) the changes in short circuit current vary from -1. 36% down to a decrease of more than -6.5% for the IBC solar cell. It has to be mentioned that the quality of the cell texture and the cell coating usually comes along with an increase for the initial cell efficiency measured against air. Therefore high efficient solar cells generate a lower coupling gain when embedded into a module.

This change in short circuit current includes the direct coupling gain due to the index matching at the cell surface and the indirect coupling gains due to re-reflection at cell surface, finger and ribbons to the eva/air interface back to cell. But in addition it also includes the reflection at the air/encapsulant surface and the absorbance losses within the encapsulation material. By re-calculating these latter effects from the measured change in short circuit current the factor for the total coupling gain at cell surface is extracted (Figure 3).

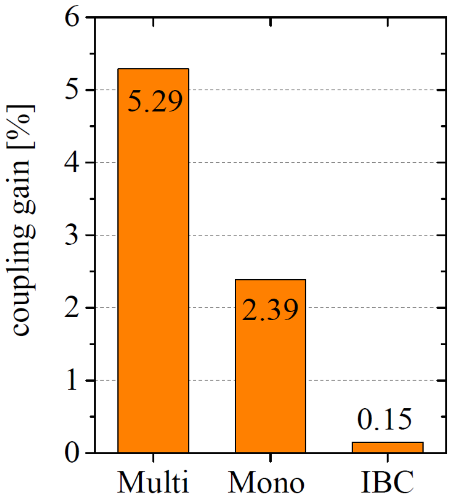

Figure 3: Calculated coupling gain for the three cell types.

The measured cell types act very differently inside a module. Higher UV spectral response and better antireflective texture lead to lower encapsulation gain. With a standard polycrystalline cell, module efficiency may be much closer to cell efficiency than with high efficiency cells.

3. Calculation of cell to module ratio and resulting module power

We setup a model which is used to predict module power and efficiency by given geometry and material parameters. These mechanisms are differentiated into losses due to inactive areas, optical losses generated by material reflectance and absorbance and optical gains generated by index matching between cell surface and encapsulant and light recycling effects.

The particular module configuration which is used for the exemplary calculation uses the following parameters:

\Module geometry:

- For Multi and Mono Cell type: 60 cell module with 10 by 6 cell matrix, 6 inch H-patterned, 27 mm border area on three sides and 35 mm on the side of the junction box, cell distance is 2 mm to the neighbouring cell
- For IBC module: 96 cell module with 12 by 8 cell matrix, 5 inch H-patterned solar cells with pseudo square edges, 27 mm border area on three sides and 35 mm on the side of the junction box, cell distance is 2 mm to the neighbouring cell

- module materials: low-iron front glass with a thickness of 3 mm, with an anti-reflective coating; EVA encapsulant, white backsheet material

The model starts with the sum of the cell power measured against air and then follows the optical losses, generated by reflection and absorption of the front materials (effect 1 to 4 in Figure 4). Further it calculated the optical gains generated by the direct and indirect coupling effects. Finally it calculates the electrical losses generated by the interconnection of the cell matrix. For the IBC module the latter losses are smaller due to the fact that the cell current is transported via the backside cell metallization to the cell edge and then is interconnected via thick copper knots.

The following table (see Table 2) gives the absolute cell to module ratios (CTM) for the three module types. The multicrystalline module generates only 3.1W power loss from cell to module while the monocrystalline module generates with 10.9Watt the highest loss. The IBC module shows the highest optical losses (sum of effects 1 to 6 in Figure 4) but generates less electrical losses, which ends up in a cell to module power loss of 10.0W.

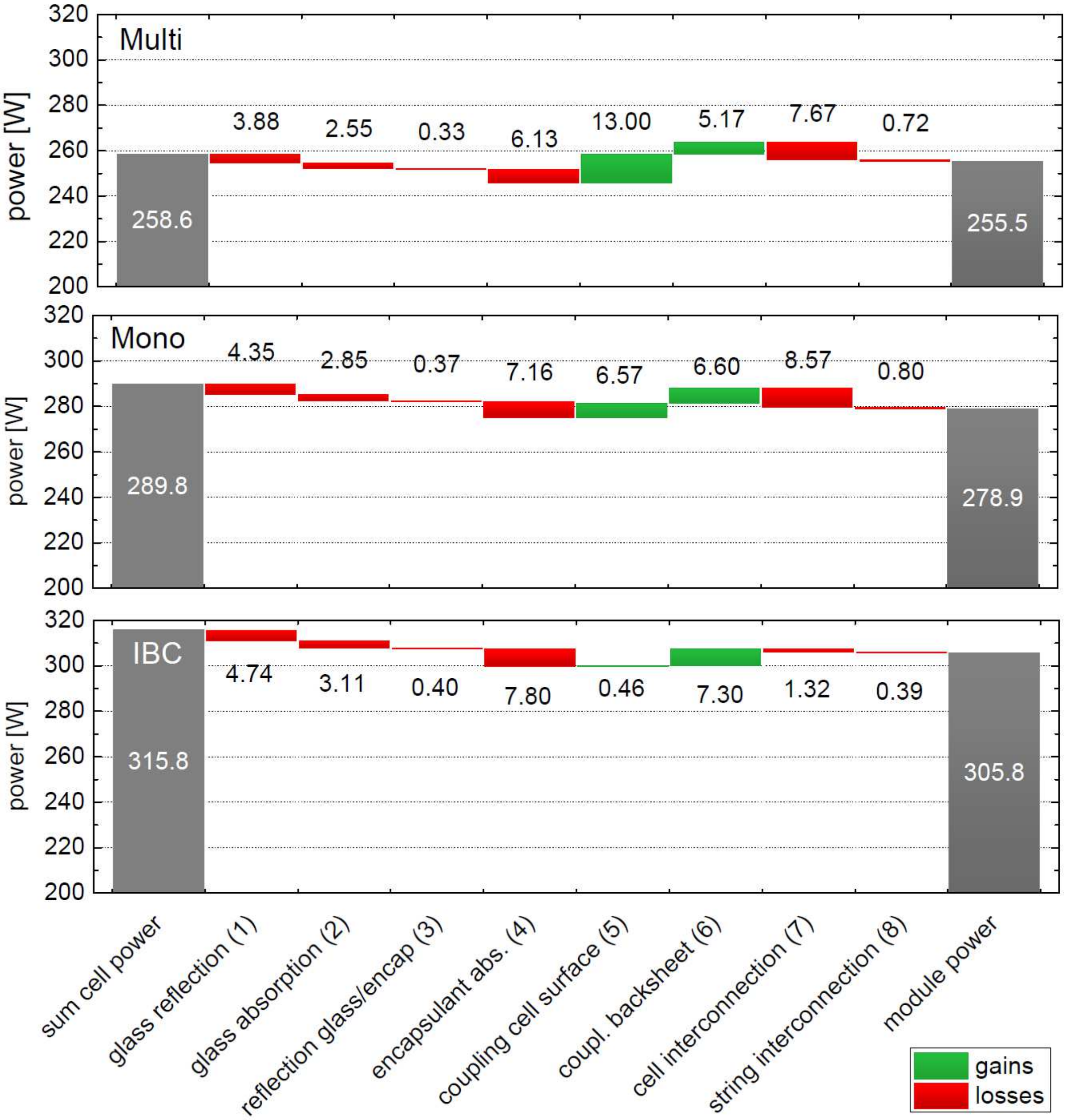

Figure 4: Calculated cell to module power losses and gains for three investigated module types.

Table 2: Overview of calculated cell to module (CTM) power losses

Module type	*Absolute CTM ratio*	*Relative CTM ratio*
Multi	3.1W	-1.2%
Mono	10.9W	-3.8%
IBC	10.0W	-3.2%

4. Conclusion

The investigated solar cells a string variance in their change in short circuit current before and after embedding from -1.36 for multicrystalline to -6.5% for IBC solar cells. This translates to a calculated coupling gain of maximum +5.3% and minimum +0.15% for IBC.

We showed that these coupling effects lead to a power loss from cell to module, calculated for an industrial common module geometry, of 3.1W for multi crystalline modules up to 10.9Watt for monocrystalline modules. This translates to relative CTM loss of minimum 1.2% and maximum 3.8%.

References

1 McIntosh, K.R., Cotsell, J.N., Cumpston, J.S., Norris, A.W., Powell, N.E., and Ketola, B.M.: 'An optical comparison of silicone and EVA encapsulants for conventional silicon PV modules: A ray-tracing study', in Editor (Ed.)^(Eds.): 'Book An optical comparison of silicone and EVA encapsulants for conventional silicon PV modules: A ray-tracing study' (2009, edn.), pp. 000544-000549

2 Haedrich, I., Eitner, U., Wiese, M., and Wirth, H.: 'Unified methodology for determining CTM ratios: Systematic prediction of module power', Solar Energy Materials and Solar Cells, 2014, 131, pp. 14-23